Volatility Uncertainty and Jumps*

Thomas Grünthaler† Hendrik Hülsbusch‡

October 28, 2019

Abstract

This paper analyzes the joint dynamics of S&P 500 jumps and volatility using option-implied information. Our results indicate that volatility is not related to the evolution of jumps but the uncertainty about volatility is. More uncertainty about future volatility shifts the return distribution to the left, such that negative price jumps are more likely and positive price jumps are less likely. We highlight the unique information content in volatility uncertainty and further show that it significantly predicts realized price jumps. Our results have strong implications for structural option pricing models as a linear link between the arrival of jumps and volatility is commonly assumed.

Keywords: Jumps, Tail Risk, Volatility, Volatility Uncertainty, Volatility-of-Volatility, Option Pricing

JEL: G12, G13

* We gratefully acknowledge very helpful comments from Yacine Aït-Sahalia, Torben G. Andersen, Tim Bollerslev, Nicole Branger, Menachem Brenner, James M. Chen, Per Mykland, Viktor Todorov, Zvi Wiener, and participants at PFMC 2018 (Paris), NYU Shanghai 2018, International Risk Management Conference 2019 (Mailand), NYU Shanghai 2019, Annual Meeting of the German Finance Association 2019 (Essen).

† School of Business and Economics, Finance Center Muenster, University of Muenster, Universitätsstr. 14-16, 48143 Münster, Germany. E-mail: thomas.gruenthaler@wiwi.uni-muenster.de. Phone: +49 251 83 22854

‡ School of Business and Economics, Finance Center Muenster, University of Muenster, Universitätsstr. 14-16, 48143 Münster, Germany. E-mail: hendrik.huelsbusch@wiwi.uni-muenster.de Phone: +49 251 83-22854

1 Introduction

The global stock market crash in October 1987 was accompanied by substantial negative price jumps of up to -22% per day. At that time, option pricing models were incapable of generating such large and sudden price movements. Especially short-term options and deep out-of-the-money puts, both of which load mostly on jump risk, were priced incorrectly and thereby offered arbitrage. To overcome this issue, the seminal work of Bates (2000) proposed a model in which jump arrivals are linked to the current volatility level. The imposed structure implies that jumps are more likely when volatility levels are high and less likely when volatility levels are low.[1] Ever since, the idea has been adapted in virtually any affine option pricing model with jumps (e.g., Pan, 2002; Eraker, Johannes, and Polson, 2003; Aït-Sahalia, Karaman, and Mancini, 2018).

A time-series of price and volatility levels justifies this idea. Figure 1 plots the S&P 500 and its realized volatility, visualizing that unusually high volatility levels are accompanied by large downside price jumps (e.g., around the financial crisis in 2008, or the U.S. downgrade in 2011). However, the recent contribution of Andersen, Fusari, and Todorov (2015, 2019) documents a strong disconnect between volatility and jump risk. Specifically, the authors show that volatility mean-reverts relatively quickly after turbulent market periods, while left-jump risk stays elevated for a longer period of time. This indicates that price jump dynamics are far more complex than previously assumed.

This paper analyzes the joint dynamics of jumps and volatility making use of option-implied information. We thus directly report how markets perceive their respective evolution and add two main findings to this line of research. Empirically, we show that uncertainty about future volatility, and not volatility itself, drives expected left and right jumps. Higher uncertainty about volatility is associated with an increase in downside risk and a decrease in upside potential. This implies that volatility uncertainty shifts the return distribution to the left such that bad economic states become more and good economic states less likely. Further, we document that uncertainty about volatility predicts realized price jumps, but not realized volatility. This suggests that information embedded in volatility uncertainty captures not only jump risk expectations and pricing but also actual realizations.

[1] Please note that we use the terms variance and volatility interchangeably throughout this article.

We evaluate our results in numerous robustness checks. Most importantly, we show that the component in volatility uncertainty that is orthogonal to volatility carries distinct information and is the main driver of jumps. Moreover, we highlight the unique informational content beyond skewness and kurtosis.

Our empirical results present a challenge to a wide range of option pricing models. We illustrate their counter-factual predictions using two specific examples. We test the stochastic volatility model with correlated jumps of Eraker (2004) that assumes a jump intensity that is linear in volatility. The model-implied results are distinctly at odds with the data. The link between volatility and jump risks is too strong and in sharp contrast to our results. Further, the model of Eraker (2004) implies a strictly negative relationship between uncertainty about volatility and both left- and right-jump risk. Higher uncertainty about volatility thus decreases downside and upside potential. We find that more uncertainty is associated with an increase in downside potential, i.e., a shift of the distribution to the left.

Next, we examine the self-exciting jump model of Kaeck (2018) that assumes an independent process for the arrival of jumps. In general, the model performs relatively well at replicating what we observe empirically. Volatility is not a significant driver of left and right jumps but volatility uncertainty is. However, the model is also not capable of reproducing an asymmetric link between volatility uncertainty and left- and right-price jumps. An increase in volatility uncertainty translates to an increase of both tails. Again, we observe a shift to the left rather than a fattening of the distribution.

Our findings are related to two strands of research. We contribute to the option pricing literature by analyzing how jump risks evolve and showing that the dynamics of jump risk need to be extended in option pricing models. Most closely related to our paper, Andersen, Fusari, and Todorov (2015) use a structural model and show that volatility and left jumps have different time-series dynamics. Further, they highlight the importance of modeling a distinct factor that drives the arrival of negative jumps to correctly price out-of-the-money put options.[2] Our contribution deviates in several ways. Most importantly, we abstract from any model specification. Instead, we let option markets speak for

[2] See Barndorff-Nielsen and Veraart (2012), Kaeck and Alexander (2013), and Kaeck (2018), amongst others, who study the effect of volatility uncertainty in option pricing models.

themselves. Additionally, we identify a tractable economic factor that drives not only the evolution of left but also of right jumps.

Our work also builds on the evolving literature on the empirical effect of volatility uncertainty on asset prices. Hollstein and Prokopczuk (2018) and Baltussen, van Bekkum, and van der Grient (2018) document that volatility uncertainty is a significant return predictor for individual stock returns. Our analysis reveals that it is also a significant predictor for extreme stock market returns that are associated with overall turbulent periods or bad economic conditions. Park (2015) and Huang, Schlag, Shaliastovich, and Thimme (forthcoming) show that volatility uncertainty explains S&P 500 and VIX option returns beyond volatility. While option returns are subject to changes in expectations, risk pricing, and realizations of the stock market, we focus on each element individually. We further build an explicit link between volatility uncertainty and price jumps.

1.1 Event Study

To illustrate our findings in a more intuitive way, Figure 2 plots quoted implied volatilities of Weekly put options (SPXW) for two different events.[3] The upper plot shows the change in implied volatilities from June 26, 2015 (solid line) to the next trading day June 29, 2015 (dotted line). Over this particular weekend, it became public that the Greek government might fail to repay its IMF loan on time. This resulted in an extreme rise in economic uncertainty and the volatility uncertainty index VVIX increased by more than 40%.

Naturally, prices of all options shift due to a higher volatility state. However, Figure 2 depicts a systematic pattern: the further the put option is out-of-the-money, the larger the price increase becomes (in terms of implied volatility). The price difference is about 12% at 97% moneyness but increases to more than 30% for the deepest out-of-the-money put. This indicates that a large rise in volatility uncertainty changes expectations about large price drops considerably. Clearly, if volatility was the driver for the shift in put prices, we would observe a symmetric upward shift over the full moneyness range. Our interpretation is further confirmed by the fact that we see symmetric price changes for

[3]Short-term options are a natural instrument to study jump as they primarily load on this source of risk (Carr and Wu, 2003).

at-the-money options ($0.97 \leq \text{m} < 1$), where changes in the jump distribution have no isolated effects.

In order to show that the pattern above does not result from a mere change in volatility, we conduct a similar event study, but use two trading days over which volatility uncertainty did not change. The lower plot shows quoted implied volatilities on January 7, 2016 (solid line) and January 8, 2016 (dotted line). Around that time, volatility uncertainty did not change at all but expected volatility, measured by the VIX, faced a relatively high absolute increase of 2.02%. Again, the higher volatility state makes puts more expensive in general. But the upward shift is symmetric across moneyness. The gap is around 3%, regardless of the moneyness considered. Consequently, there is no isolated effect on the left tail as opposed to the event in June 2015.

The remainder of the work is organized as follows: Section 2 introduces the option-implied measures, while Section 3 describes the data. Section 4 discusses the results of our empirical analysis. We study the performance of option pricing models in Section 5 before the last section concludes.

2 Option-Implied Risk Measures

Our analysis is primarily based on option-implied risk measures. In this section, we specify how to characterize the return distribution from option prices. Under the risk-neutral probability measure $\mathbb{Q}$, assume that the stock price S follows a jump-diffusion-process of the form

$$\frac{dS_t}{S_{t-}} = (r - \delta)\, dt + \sigma_t dW_t^S + \int_{\mathbb{R}} (e^x - 1)\, \widetilde{\mu}(dt, dx), \tag{1}$$

$$d\sigma_t^2 = \alpha_t^\sigma dt + \eta_t dW_t^\sigma + \int_{\mathbb{R}} Z_t^\sigma(x) \widehat{\mu}(dt, dx), \tag{2}$$

where r is the short-rate and δ the continuous dividend yield, σ_t the volatility process with drift α^σ, jumps $Z_t^\sigma(x)$, and stochastic volatility-of-volatility η_t. The two Brownian motions W^S and W^σ might be correlated and $\widetilde{\mu}(dt, dx) = \mu(dt, dx) - dt\nu_t(dx)$ is a compensated jump process.[4] The variance or quadratic variation of the stock price over time-interval $[t, t + \tau]$ can be decomposed into two

[4] In conventional models the volatility process is often parameterized mean-reverting with drift $\alpha_t^\sigma = \kappa^\sigma (\theta^\sigma - \sigma_t)$, volatility process $\eta_t = \sqrt{\sigma_t}$, and jump-size $x \sim \text{Exp}(\mu^\sigma)$.

components:

$$\mathrm{QV}_t^{t+\tau} = \underbrace{\int_t^{t+\tau} \sigma_s^2 ds}_{\mathrm{CV}_t^{t+\tau}} + \underbrace{\int_t^{t+\tau} \int_{-\infty}^{\infty} x^2 \mu(ds, dx)}_{\mathrm{JV}_t^{t+\tau}}. \tag{3}$$

The first component, $\mathrm{CV}_t^{t+\tau}$, measures the stock's variation due to continuous movements. The second, $\mathrm{JV}_t^{t+\tau}$, captures the variation stemming from positive and negative jumps in the price path (discontinuous movements). Hence, $\mathrm{JV}_t^{t+\tau}$ measures variations that contribute to the left and right tail of the return distribution.

2.1 Volatility and Volatility Uncertainty

Amongst others, Bondarenko (2014) and Andersen, Bondarenko, and Gonzalez-Perez (2015) show that the risk-neutral expectation of the quadratic variation $\mathbb{E}_t^{\mathbb{Q}}\left[\mathrm{QV}_t^{t+\tau}\right]$ can be exactly replicated by a portfolio of options

$$\mathbb{E}_t^{\mathbb{Q}}\left[\mathrm{QV}_t^{t+\tau}\right] = 2e^{\int_t^{t+\tau} r_s ds}\left(\int_0^{\infty} \frac{O_t^{\tau}(K)}{K^2} dK\right), \tag{4}$$

where $O_t^{\tau}(K)$ are prices of OTM options on the S&P 500 with time-to-maturity τ and strike price K. Under very general assumptions, this replication is robust to jumps in the price process.[5] As is standard, we estimate the expected volatility risk over 30 days and label it

$$\mathrm{Vol}_t^2 = \frac{1}{30\mathrm{D}} \mathbb{E}_t^{\mathbb{Q}}\left[\mathrm{QV}_t^{t+30\mathrm{D}}\right], \tag{5}$$

which is the well-known volatility index VIX.[6] Using a similar approach, we proxy volatility uncertainty (volatility-of-volatility) by the expected variation of Vol_t^2. The main difference to above is the

[5] Bondarenko (2014) shows that the only necessary assumption is that the realized variance is filtered using *weighted* returns. Thus, $\mathbb{E}_t^{\mathbb{Q}}\left[\mathrm{QV}_t^{t+\tau}\right] = \mathbb{E}_t^{\mathbb{Q}}\left[RV^{\omega}\right] = 2\mathbb{E}_t^{\mathbb{Q}}\left[\sum_i (r_i^s - r_i^c)\right]$, where $r_i^s = \frac{F_i - F_{i-1}}{F_{i-1}}$ is the simple arithmetic return and $r_i^c = \log(F_i) - \log(F_{i-1})$ is the log-return.

[6] Note that we abstract from the CBOE's calculation methodology due to potential biases (Andersen, Bondarenko, and Gonzalez-Perez, 2015).

underlying used for the option portfolio, which is a future on volatility (VIX) and not the S&P 500.[7] The price of the volatility future with maturity τ is given by

$$F_t^{\text{Vol},\tau} = \mathbb{E}_t^{\mathbb{Q}}\left[\text{Vol}_{t+\tau}\right] = \mathbb{E}_t^{\mathbb{Q}}\left[\sqrt{\int_{t+\tau}^{t+\tau+30\text{D}} (dS_u)^2\, du}\right]. \tag{6}$$

The expected QV of the volatility future can be expressed by a portfolio of VIX options

$$\mathbb{E}_t^{\mathbb{Q}}\left[\text{QV}_t^{\text{Vol},t+\tau}\right] = 2e^{\int_t^{t+\tau} r_s ds}\left(\int_0^{\infty} \frac{O_t^{\text{VIX},\tau}(K)}{K^2} dK\right), \tag{7}$$

where $O_t^{\tau}(K)$ are prices of OTM VIX options with strike K. Again, we estimate volatility uncertainty for 30 days and define

$$\text{VolVol}_t^2 = \frac{1}{30\text{D}}\mathbb{E}_t^{\mathbb{Q}}\left[\text{QV}_t^{\text{VIX},t+30\text{D}}\right]. \tag{8}$$

2.2 Tail Risk

For measuring the jump-induced return variation $\mathbb{E}_t^{\mathbb{Q}}\left[\text{JV}_t^{t+\tau}\right]$, we rely on the methodology of Bollerslev, Todorov, and Xu (2015). We distinguish between negative (LJV) and positive (RJV) jumps and define

$$\text{LJV}_t^{t+\tau} \equiv \int_t^{t+\tau}\int_{-\infty}^{-c_t} x^2 \nu_s(dx)ds, \quad \text{RJV}_t^{t+\tau} \equiv \int_t^{t+\tau}\int_{c_t}^{\infty} x^2 \nu_s(dx)ds. \tag{9}$$

Here, ν_t is the jump intensity process and x^2 the (squared) jump size. We only consider jumps that are larger than a time-varying cut-off $c_t > 0$. As in Bollerslev and Todorov (2014), we assume that the jump intensity process $\nu_t(dx)$ is defined by

$$\nu_t(dx) = \left(\phi_t^+ \times e^{-\alpha_t^+ x}\mathbf{1}_{\{x>0\}} + \phi_t^- \times e^{\alpha_t^- x}\mathbf{1}_{\{x<0\}}\right). \tag{10}$$

[7] Other empirical studies that explore the effect of volatility uncertainty using the same methodology are, for instance, Hollstein and Prokopczuk (2018), Baltussen, van Bekkum, and van der Grient (2018), and Huang, Schlag, Shaliastovich, and Thimme (forthcoming).

The parameters $\phi^{\pm}$ govern the *levels* of the tails, that is, their thickness. Parameters $\alpha^{\pm}$ are the *shapes* of the respective tail and control the speed of decay. The larger $\alpha^{\pm}$, the faster the tail of the return distribution decays and therefore the less severe is the priced jump risk. We explicitly assume a separation between negative and positive jump intensity parameters, allowing for independent variations and hence a more realistic modeling of the tails.[8] Under this specification, the expected jump variations in Equation (9) can be expressed by

$$\mathrm{RJV}_t^{t+\tau} = \tau\phi^{+}e^{-\alpha_t^{+}|c_t|}\left(\alpha_t^{+}c_t\left(\alpha_t^{+}c_t+2\right)+2\right)/(\alpha_t^{+})^3, \tag{11}$$

$$\mathrm{LJV}_t^{t+\tau} = \tau\phi^{-}e^{-\alpha_t^{-}|c_t|}\left(\alpha_t^{-}c_t\left(\alpha_t^{-}c_t+2\right)+2\right)/(\alpha_t^{-})^3. \tag{12}$$

Bollerslev and Todorov (2014) demonstrate that all four jump parameters can be estimated in a two-step procedure. First, to estimate the decay $\alpha^{\pm}$, the authors rely on the result that the log-price of deep-OTM put (call) options O_t increases (decreases) linearly in the log-moneyness k_t^i and show that

$$\widehat{\alpha_t}^{\pm} = \underset{\alpha_t^{\pm}}{\arg\min}\frac{1}{N_t^{\pm}}\sum_{i=1}^{N_t^{\pm}}\left|\frac{\log\left(O_t^{\tau}\left(k_t^i\right)\right)-\log\left(O_t^{\tau}\left(k_t^{i-1}\right)\right)}{\left(k_t^i-k_t^{i-1}\right)}-\left(1\mp\alpha_t^{\pm}\right)\right|, \tag{13}$$

where $N_t^{\pm}$ denotes the respective number of calls and puts used during the estimation. Given this estimate, the level parameter can be determined by

$$\widehat{\phi_t}^{\pm} = \underset{\phi_t^{\pm}}{\arg\min}\frac{1}{N_t^{\pm}}\sum_{i=1}^{N_t^{\pm}}\left|\log\left(\frac{e^{\int_t^{\tau}r_s ds}O_t^{\tau}\left(k_t^i\right)}{\tau F_{t-}^{\tau}}\right)-\left(1\mp\widehat{\alpha}_t^{\pm}\right)k_t^i \right. \tag{14}$$
$$\left. +\log(\widehat{\alpha}_t^{\pm}\mp 1)+\log\left(\widehat{\alpha}_t^{\pm}\right)-\log\left(\phi_t^{\pm}\right)\right|.$$

2.3 Skewness

Following Kozhan, Neuberger, and Schneider (2013), we estimate risk-neutral skewness as the difference between the quadratic variation and entropy. Specifically, quadratic variation is defined as in

[8] Given that OTM put options have different dynamics than OTM call options, the separation is reasonable. See also the discussion in Bollerslev, Todorov, and Xu (2015).

Equation (4) while entropy is given

$$\mathbb{E}_t^{\mathbb{Q}}\left[\mathrm{v}_t^{t+\tau}\right] = 2e^{\int_t^{t+\tau} r_s ds}\left(\int_0^{\infty} \frac{O_t^{\tau}(K)}{KF_t^{\tau}} dK\right). \tag{15}$$

Equation (4) is more sensitive to the tails of the return distribution (especially OTM puts) because all option prices O_t^{τ} are weighted inversely with their squared strike K. In contrast, Equation (15) weighs option prices by the strike times the forward price F_{τ}. As derived by Kozhan, Neuberger, and Schneider (2013), the scaled difference between both measures is the risk-neutral expected skewness:

$$\mathrm{SKEW}_t^{t+\tau} = 3\,\frac{\mathrm{v}_t^{t+\tau} - \mathrm{QV}_t^{t+\tau}}{(\mathrm{QV}_t^{t+\tau})^{3/2}}. \tag{16}$$

2.4 Empirical Implementation

The estimation of option-implied risk measures relies on a continuum of option prices and in some cases on fixed times-to-maturity. These criteria are not always met by the available option data. To overcome these issues we employ the basic interpolation techniques from Jiang and Tian (2005, 2007). However, we refrain from extrapolating the strikes to avoid obscuring the tails.

To construct the tail risk measures we need to define a certain range of options considered and a cut-off for the jump-size c_t. We closely follow Bollerslev, Todorov, and Xu (2015) and use puts with moneyness[9] $m \leq -2.5$ and calls with $m \geq 1$ as well as a time-varying cut-off $c_t = 9.11 \times \mathrm{IV}^{\mathrm{ATM}}$. Assuming a current $\mathrm{IV}^{\mathrm{ATM}}$-level of 30% this corresponds to a weekly jump of approximately 2%.[10]

We estimate the tail risk measures on a weekly basis. Just as Bollerslev, Todorov, and Xu (2015), we choose this horizon to mitigate noise due to liquidity or market frictions. In order to be in line with the frequency of the tail measures, we aggregate our other measures to weekly averages. This leaves us with 485 weeks of observations in total.

[9] See Equation (17) for the definition of moneyness.

[10] The value for the cut-off rule is determined by median implied volatility of the furthest OTM option available in any given week. This value, of course, is somewhat arbitrary. However, the need for omitting small price jumps is imposed by the available options, which only allow for estimating the impact of large jumps. See the discussion in Bollerslev, Todorov, and Xu (2015).

3 Data

We obtain S&P500 and VIX options from OptionMetrics for the period from January 3, 2007 to April 29, 2016.[11] The option data comprises daily end-of-day bid and ask quotes, as well as trading volume, open interests, and implied volatilities. We apply the same basic filters as in Andersen, Fusari, and Todorov (2017) and discard SPX and VIX options which violate basic no-arbitrage bounds or have zero bid-prices. In addition, we follow Bollerslev, Todorov, and Xu (2015) for SPX options and delete contracts for which the mid price does not decrease in the strike. We restrict our sample to SPX options with time-to-maturity of no more than 45 days.[12] Our filters leave us with 2.2 million SPX option prices and 0.86 million VIX option prices.

Next, we define moneyness m as

$$m = \frac{\log(\frac{K}{S})}{\sqrt{\tau} \times \mathrm{IV}^{\mathrm{ATM}}}, \tag{17}$$

where K is the strike of the option, S is the price of the underlying, τ the time-to-maturity, and $\mathrm{IV}^{\mathrm{ATM}}$ is the average implied volatility of an ATM put and ATM call. The normalization of log-moneyness yields a consistent measure of moneyness across different horizons. Table I shows the relative trading volume, open interest, and the bid-ask spread across different moneyness buckets for SPX options. The trading activity mainly concentrates on deep-OTM puts ($m \leq -4$) and deep-OTM calls ($m > 4$). The trading volume make up 36% and 13%, respectively, of the overall volume. The combined open interest equals 63% of the total open positions. The median bid-ask spread of 4% is the smallest for OTM put options. For OTM calls, the spreads are slightly larger with values of 5% to 7%. Overall the table documents high liquidity of deep-OTM SPX put and call options with maturities of less than 45 days. Consequently, the data are adequate to study both tails of the expected return distribution, which require high liquidity to be estimated correctly.

[11] The start date of our sample is dictated by the liquidity of VIX options.

[12] In contrast to Bollerslev, Todorov, and Xu (2015), who exclude options with time-to-maturity of less than 9 days, we choose to include all short-term options in order to incorporate the full information from SPX weeklies.

4 Empirical Results

Albeit option pricing models commonly assume a strong link between volatility and jumps, recent evidence from the model of Andersen, Fusari, and Todorov (2015, 2019) documents a strong discrepancy in their time-series. This suggests that price jumps dynamics are more complex than previously assumed. In this section, we analyze the joint behavior of price jumps and high-order moments by letting option prices completely speak for themselves, thereby abstract from any strong structural assumptions.

4.1 Descriptives

Figure 3 and 4 display the weekly time-series of left-jump variation (LJV) and right-jump variation (RJV) in comparison to volatility, volatility uncertainty, and skewness. We note an obvious co-movement among expected left-tail risk, volatility, and volatility uncertainty during turbulent market conditions. This is particularly evident around the financial crisis in 2009, the Flash Crash in mid 2010, and the U.S. downgrade in 2011. Skewness, on the other hand, seems to have dynamics that are relatively independent. The negative swings in skewness around 2007, 2009, and 2011 do not coincide with any of the other measures. In contrast to downside risk, the series for upside potential (RJV) is quite different. While the level is close to 0% at the peak of the financial crisis, significant spikes in RJV emerge thereafter. Generally, those spikes originate when volatility is at a normal level and thus when markets are calm. Noteworthy, the two large increases in RJV around the end of 2013 and 2014 (mid-term election) occurred right after volatility uncertainty sharply drops.

The visual impression is confirmed by the descriptive statistics reported in Table II. We observe that the level of the left tail is (i) strongly positively correlated to volatility (79%) and volatility uncertainty (43%), (ii) weakly correlated to skewness (7%), and (iii) independent of the right tail (3%). The correlation between the level of RJV and the other risk measures is negative, albeit of varying degree. Interestingly, (i) volatility uncertainty (-23%) has a stronger impact than volatility (-12%) and (ii) skewness seems to have a more pronounced effect on RJV (-23%) than on LJV (7%).

Turning to the other moments, we note that the levels of all measures exhibit very strong weekly

autocorrelations. The tail measures RJV and LJV have autocorrelations of 60% and 79%, respectively. The correlations are even higher for skewness (82%), volatility uncertainty (82%), and volatility (95%). Drawing proper inferences with such high autocorrelations might be problematic. Therefore, we report descriptives for weekly differences in Panel B of Table II. Indeed, a slightly different picture emerges. We document that (i) for LJV changes, the correlation to volatility uncertainty (29%) is now stronger than to volatility (26%) and (ii) changes in skewness have a negative relation to changes in either tail risk. Overall, our results indicate that changes in volatility and volatility uncertainty have a positive impact on left-tail risk. That is, a higher expected volatility or volatility uncertainty increases the expectation about negative price jumps. Positive price jumps, in contrast, are rather solely driven by changes in volatility uncertainty. An increase in volatility uncertainty decreases expectations about positive price jumps in the future.

4.2 Drivers of Expected Tail Risk

To explore the drivers of expected tail risk in more detail, we run regressions of the form

$$\Delta\text{Jump Measure}_t = \alpha + \beta \Delta X_t + \epsilon_t.$$

In this setup, ΔJump Measure is the weekly difference in either RJV or LJV, and X_t is a set of explanatory variables. We include the weekly difference of Vol^2, VolVol^2 and SKEW in the univariate regressions and further run multivariate regressions. To ensure comparability we normalize all input variables by their standard deviation.

As documented in Table II, the correlation between changes in VolVol^2 and Vol^2 is fairly high (44%). Hence, both measures share similar (linear) information. We disentangle information and orthogonalize our measures for the multivariate analysis. Albeit it is arguable in which direction to orthogonalize, we define $\text{VolVol}^{2,\perp}$ as the intercept γ plus residual η_t from following regression:

$$\text{VolVol}_t^2 = \gamma + \phi\, X_t + \eta_t.$$

Here, X_t is the Vol^2, SKEW, or both. Using this routine, we explicitly remove information out of our volatility uncertainty measure and only use the incremental information for our analysis.[13]

Table III reports results of the regressions for the innovation in LJV. Our results show that expected volatility uncertainty risk is highly important for the left part of the expected return distribution. For the VolVol^2, we find a coefficient of 0.2943 with a t-stat of 3.44 and an R^2 of 8.45%. Thus, a one standard deviation increase in volatility uncertainty leads to an increase of about one-third standard deviations in expected left jumps. The effect is less pronounced and significant for expected volatility. For the Vol^2, the beta of 0.2578 is only significant at the 10% level. However, the multivariate analysis reveals that the significance of the Vol^2 in (1) is driven by its correlation to VolVol^2. Despite we assign Vol^2 shared linear information in (3), the coefficient of 0.1954 is not distinguishable from 0, i.e., not significant. The unique information provided by $\text{VolVol}^{2,\perp}$, on the other hand, yields important insights about expected left jumps. The coefficient of 0.2025 is highly significant with a t-stat of 3.01.

When we add skewness as a control in (4), our result that expected volatility uncertainty provides important information about expected left jumps does not change at all. In fact, the coefficient for $\text{VolVol}^{2,\perp}$ increases to 0.3156 with a higher significance than in (3). Interestingly, SKEW is also highly informative about changes in expected negative price jumps. The negative slope indicates that left jumps are perceived to be less likely when skewness increases towards gaussianity. This mechanism makes sense intuitively. Most importantly, the adjusted R^2 is considerably higher in (4) compared to (3). Therefore, we attribute skewness to explain more variation in expected left-tail risk than volatility does.

Regression (5) includes all three explanatory variables and we observe similar results as above. Volatility uncertainty and skewness are highly significant while volatility is only borderline significant. This is striking given our orthogonalization. Overall, our results show that the innovations in the left tail are only explained by innovations in expected volatility uncertainty as well as skewness and do not coincide with changes in expected volatility. When expected volatility uncertainty increases, the possibility of large, negative price movements is perceived to be more likely.

Next, we turn to the analysis of the right tail as reported in Table IV. The regression results show that

[13] We note that orthogonalizing the other way would strengthen the results below.

an increase in volatility uncertainty has a sizable negative effect on expected positive jumps in the stock market. For VolVol^2 in (2), we find a coefficient of -0.1220 that is significant at the 1% level. Thus, higher expected volatility uncertainty is associated with less future upside potential. It indicates that uncertainty about future volatility shifts the whole return distribution. Higher uncertainty translates to more downside risk and less upside potential, i.e., shifts the distribution to the left. Less uncertainty, in contrast, is associated with less downside risk and more upside potential thus shifts the distribution to the right.

Changes in expected volatility have almost no impact on the right tail. The coefficient for Vol^2 is -0.0515 and is only significant at the 10% level. In (3), we show that the significance is due to the fact that Vol^2 partly carries same information. Orthogonal volatility uncertainty expels the significance of Vol^2 completely. We further note that skewness also carries distinct information for the right tail of the return distribution. This is suggestive given its t-stat of 1.88 and the sharp increase in the explained variation. Surprisingly, the coefficient is also negative as for LJV. Thus, a higher skewness does not only reduce LJV but also RJV. Our finding that volatility itself is not important for expected right-tail risk is confirmed in (5). In fact, the R^2 even decreases compared to (4). All in all, we find that changes in volatility uncertainty are related to changes in expected upside jumps, but changes in expected volatility are not. The higher expected volatility uncertainty, the less probable are extreme upside movements of the stock price.

Table V reports the results of further robustness checks. Column (1) and (3) show that our results are not driven by outliers as we exclude the prime of the recent financial crisis in this subsample (2010-2016). Coefficients, statistical significance, and explained variation are similar in magnitude. We also test whether kurtosis, a higher-order moment that is naturally related to jumps, changes our results (colum (2) and (4)). Again, our interpretation that volatility uncertainty increases left tail risk and decreases right tail risk does not change at all.[14]

[14]We follow Bakshi, Kapadia, and Madan (2003) for the estimation of kurtosis.

4.3 Predicting Realized Price Jumps

To emphasize our finding that volatility uncertainty is tied to price jumps, we now explore the ability of expected volatility and volatility uncertainty to forecast realized risks estimated from high-frequency return data. We test whether the option-implied measures predict realized volatility and/or realized price jumps. We measure realized volatility in standard fashion and sum up 5-minute log returns. We define realized price jumps as the difference between realized volatility and tripower variation. Pioneered by Barndorff-Nielsen, Shephard, and Winkel (2006), tripower variation and other multi-power variation statistics are jump-robust estimates of the integrated variance (the continuous variation $\text{CV}_t^{t+\tau}$ from Equation (3)). Hence, the difference between realized volatility and tripower variation effectively isolates the impact of realized jumps.

In contrast to standard practice in the predictive literature, we rely on shorter horizons for our analysis. Because jumps are transitory and quickly vanish out, this choice is reasonable. We run the regressions using weekly data for the horizons of 1 week up to roughly 6 months into the future. All variables that we include correspond to weekly averages and are not aggregated over the full prediction horizon. If we set time $t = 0$ and want to predict $t + h = 2$ then our predictor in t (e.g. the VVIX_0) forecasts the weekly average of the realized risk over week 2 but not over the full horizon (week 1 and week 2).[15]

A visualization of our results can be found in Figure 5. The right panel shows significance levels of our two predictors while in the left panel, we plot the total R^2 obtained from

$$\text{Realized Risk}_{t+h} = \gamma + \beta_{Vol}\,\text{Vol}_t^2 + \beta_{VolVol}\,\text{VolVol}_t^2 + \epsilon_t, \tag{18}$$

and compare it to the R^2 from the univariate regression with VolVol^2 as the predictor.

For realized volatility, the total predictive power of volatility and volatility uncertainty is almost 70% for the next week and reduces steadily to approx. 10% for the realization six months later. However, the forecast ability almost exclusively comes from expected volatility. Expected volatility uncertainty explains only little of the variation of realized volatility for horizons up to 5 weeks and nothing

[15] This set-up reduces the obtained R^2 per construction compared to the standard approach in the predictive literature (the aggregation over the horizon). Yet, it does not alter the interpretation of our results.

thereafter. In fact, the right panel shows that its ability to significantly predict realized volatility vanishes out after 1 week. In contrast, expected volatility stays a highly significant predictor for all horizons. This signifies a large discrepancy in the information content of both variables for predicting future realized risk.

Strikingly, we find opposite roles when we predict realized price jumps. The predictive power is relatively high for the short-term (R^2 of 30%) and decreases with longer prediction horizons. Out of the 30% explained variation, 24% alone come from expected volatility uncertainty. This proportion increases for longer horizons and after 8 weeks almost 100% of the R^2 is attributable to the prediction power of volatility uncertainty. Throughout all horizons, volatility uncertainty's ability to forecast realized price jumps is consistently better, i.e., has a higher R^2 in univariate regressions. The picture is confirmed by the t-statistics in the right panel. Volatility uncertainty stays a significant predictor of jump realizations for up to 16 weeks and Vol for only six. Our evidence highlights that volatility uncertainty contains valuable information for future realized jumps, and that this information is not spanned by volatility itself. This is remarkable given that almost any option pricing model links jump risk directly to volatility.

5 Option Pricing Models

In the previous section, we show that volatility uncertainty is significantly related to jump risk, not only in terms of expectations but also realizations. Further, we document that the evolution of jump risk is largely independent of volatility itself. It is challenging for option pricing models to meet our findings given that many assume the jump intensity to be linked to volatility. That is,

$$\lambda_t = \lambda_0 + \lambda_1 V_t + \dots \tag{19}$$

Naturally, this induces a strong relation between volatility and jumps. To highlight the potentially conflicting implications of most models with our empirical findings, we test the performance of two option pricing models. First, we use the SVSCJ model of Eraker (2004) which features stochastic

volatility and correlated jumps in volatility and stock prices. The jumps are assumed to depend on the current level of local volatility. Next, we examine the structural 3-factor model of Kaeck (2018) which incorporates two additional factors: central tendency level m_t and jump intensity factor λ_t. In contrast to standard models, the jump intensity λ_t follows a separate process that can jump itself. Hence, the model exhibits self-exciting jumps.

5.1 The SVSCJ model of Eraker (2004)

The SVSCJ model is mainly built on the affine framework of Duffie, Pan, and Singleton (2000). Under the risk-neutral measure $\mathbb{Q}$, the model is specified as

$$\frac{dS_t}{S_t} = (r - \mu)dt + \sqrt{V_t}dW_t^{S,\mathbb{Q}} + dJ_t^{S,\mathbb{Q}}, \tag{20}$$

$$dV_t = \kappa^{\mathbb{Q}}(\theta^{\mathbb{Q}} - V_t)dt + \sigma_V\sqrt{V_t}dW_t^{V,\mathbb{Q}} + dJ_t^{V,\mathbb{Q}}, \tag{21}$$

where r is the risk-free rate, μ the jump compensator, $dW_t^{i,\mathbb{Q}}$ the correlated Brownian motions, and $dJ_t^{i,\mathbb{Q}} = Z_t^i dN_t^i$ the jump terms with jump magnitude Z_t and Poisson process N_t. Both Poisson processes have a stochastic arrival rate λ_t that follows

$$\lambda_t = \lambda_0 + \lambda_1 V_t. \tag{22}$$

In contrast to arrival rates that are kept constant, this specification implies time variations such that jumps occur more frequently during turbulent times. Eraker (2004) further allows for a cross-relation between jumps in volatility and jumps in the stock price. The conditional jumps in S_t are given by

$$Z_t^S \mid Z_t^V \sim N(\mu_S + \rho_J Z_t^V, \sigma_J). \tag{23}$$

Consequently, stock prices can only jump when volatility jumps, and the size of the stock price jump depends on the size of the volatility jump. It is likely that this model falsely predicts a strong link between volatility risk and the tails, as jumps are closely related through their arrival probability and

magnitude.

In terms of volatility uncertainty, the model implies

$$(dV_t)^2 = V_t \left(\sigma_V^2 + \mathbb{E}_t^{\mathbb{Q}} \left[\left(Z_t^V \right)^2 \right] \right) dt. \tag{24}$$

Obviously, volatility (V_t) and volatility uncertainty $(dV_t)^2$ are driven by the same elements: the current volatility level V_t, time-invariant volatility-of-volatility σ_V^2, and volatility jumps. Therefore, we expect volatility uncertainty to be related to model-implied jumps but not to provide meaningful incremental information.

We test the model's capability to match our empirical findings by conducting a simulation study. Our simulation is based on the following steps: First, we solve the model in closed-form for its risk-neutral variance expectation. The solution is taken to invert the empirically observable VIX in order to extract the latent state variable V_t.[16] Afterwards, we calculate model-implied call and put prices for the S&P500 and the VIX. The option prices are further translated into the same risk measures we used before. We repeat this exercise for the 485 weekly observations of our empirical section and carry out the same analysis. We rely on the model parameters estimated in Eraker (2004) for our procedure.

Table VI reports the results and confirms that the model does not match the empirical evolution of the tails. We find that changes in left jumps are mainly driven by volatility. The slope is very steep with a value of 0.8102 and thus an increase in volatility by one standard deviation almost translates uniformly to left-tail risk. The R^2 of 65% is also counter-factually large and roughly ten-times larger than in the data. However, the model has a harder time replicating the relationship between volatility uncertainty and the left tail. (2) shows that the coefficient is negative. That is, an increase in volatility uncertainty leads to a decrease in left-jump risk. This is particularly at odds with our results.

In terms of upside potential (RJV), our results indicate that the right tail is also mainly driven by volatility and not volatility uncertainty. This is suggested by the larger R^2 and the fact that

[16] In affine option pricing models, the squared VIX for maturity τ can be expressed as $\text{VIX}_t^2(\tau) = A(\tau) + B(\tau)' X_t$, where X_t is the state variable vector. For example, Bardgett, Gourier, and Leippold (2016) use this inversion methodology to filter state variables.

he absolute coefficient of volatility (0.12) is larger than the coefficient for volatility uncertainty (-0.08). The multivariate regression in (6) confirms this. The model-implied relation between volatility uncertainty and upside potential is predicted correctly, but not as strong as in the data. In fact, (6) shows that volatility uncertainty is not a significant driver in the model.

Overall, coupling the jump intensity to V_t results in two counter-factual implications: First, volatility is the main driver of jump risks in the model. Second, the relation between volatility uncertainty and both tails is strictly negative, indicating that a rise in uncertainty shrinks both tails of the distribution. Empirically, we find that higher uncertainty about volatility shifts the distribution to the left, thereby increasing downside risk and decreasing upside potential. The simulation study confirms that a different specification for the jump intensity is necessary.

5.2 The 3-factor model of Kaeck (2018)

Based on a model-free analysis of VIX options, in which a significant premium for volatility uncertainty is found, Kaeck (2018) proposes to model a separate process for the jump intensity. The dynamics of the model are given by

$$\frac{dS_t}{S_t} = (r - q - \mu)dt + \sqrt{V_t}dW_t^{S,\mathbb{Q}} + dJ_t^{\lambda,\mathbb{Q}} \tag{25}$$

$$dV_t = \kappa_V^{\mathbb{Q}}(m_t - V_t)dt + \sigma_V\sqrt{V_t}(\rho dW_t^{S,\mathbb{Q}} + \sqrt{1-\rho^2}dW_t^{V,\mathbb{Q}}) + dJ_t^{\lambda,\mathbb{Q}}, \tag{26}$$

$$dm_t = \kappa_m^{\mathbb{Q}}(\theta_m^{\mathbb{Q}} - m_t)dt + \sigma_m\sqrt{m_t}dW_t^{m,\mathbb{Q}}, \tag{27}$$

$$d\lambda_t = \kappa_l^{\mathbb{Q}}(\theta_l^{\mathbb{Q}} - \lambda_t)dt + \sigma_l\sqrt{\lambda_t}dW_t^{l,\mathbb{Q}} + dJ_t^{\lambda,\mathbb{Q}}, \tag{28}$$

where q are dividends, $dW_t^{i,\mathbb{Q}}$ some independent Brownian motions, m_t the stochastic mean-reversion level for V_t, and $J_t^{\lambda,\mathbb{Q}}$ the jump terms in which the jump sizes are not correlated. λ_t denotes the stochastic jump intensity process that controls the jump activity in the stock price and in volatility. Moreover, λ_t is the jump intensity for jumps in itself. Hence, high levels of λ_t not only assure jump activity in S_t and V_t but also in λ_t itself, which, in turn, makes further jumps more likely (self-

exciting).[17] This modeling choice imposes strong correlations among all processes that can jump. The relationship becomes more obvious when we look at the model-implied volatility uncertainty, given by

$$(dV_t)^2 = \left(\sigma_V^2 V_t + \lambda_t \mathbb{E}_t^{\mathbb{Q}}\left[\left(Z_t^l\right)^2\right]\right) dt. \tag{29}$$

In contrast to Equation (24), uncertainty about volatility is also subject to the evolution of λ_t. The same process governs jumps in S_t. Hence, λ_t is directly related to volatility uncertainty as well as jumps. Therefore, we expect a stronger relationship between tail risk and volatility uncertainty as well as a weaker to volatility.

Table VII reports the results of the simulation study. For downside risk (LJV), we find close-to-empirics results. We note that Vol^2 coefficient in (1) is statistically indistinguishable from 0 and the R^2 is negative. Volatility uncertainty, on the other hand, has a slope that is close to what we find empirically, in terms of the direction and magnitude. The multivariate regression does not change our conclusion that volatility uncertainty is the main driver in the model, albeit Vol^2 is significantly negatively related to downside risk. We attribute this to our orthogonalization routine.

Regressions (4) to (6) report the results for upside potential (RJV) and show that the right tail of the return distribution only loads on volatility uncertainty. However, the loading is positive which is in sharp contrast to our findings. An increase in VolVol^2 does not shift the distribution to the left but rather extends it. Hence, the model is incapable of reproducing a shift of the return distribution.

In general, the model proposed by Kaeck (2018) is more realistic and matches our findings better: The innovations in either tail measure are solely driven by volatility uncertainty. The relation to the left tail is modeled almost perfectly. The right tail, however, has a significant positive relationship whereas we find a negative. The strictly positive relation exists because λ_t drives both the jump in the stock price and the model's volatility uncertainty. Decoupling the jump intensity of positive and negative jumps would solve this shortfall.

[17] See Carr and Wu (2017) who study the behavior of self-exciting jump models.

6 Conclusion

This paper analyzes the relationship between jumps and volatility for the S&P 500. Our analysis is model-free and fully based on observable option prices. Contrary to the common approach of modeling jumps, our analysis uncovers a sharp disconnect between their evolution and volatility. However, we show that uncertainty about future volatility provides significant insights about the dynamics of jumps. An increase in volatility uncertainty translates to an increases in downside risk and a decreases in upside potential. Consequently, higher volatility uncertainty shifts the expected return distribution to the left. We emphasize our main finding by an event studies and additionally highlight the relevance of volatility uncertainty by showing its predictive power for realized price jumps. Moreover, we document an unique informational content beyond skewness and kurtosis

Our findings present a challenge for many option pricing models. We show that the usual structure imposed to the arrival of jumps, namely linear in volatility, results in unreasonable predictions that are in sharp contrast to our empirical findings. A model that assumes an independent process for the arrival of jumps performs relatively well. However, it still has problems to meet the asymmetric relationship between volatility uncertainty and jumps. While the model consistently shrinks or fattens the return distribution, we observe shifts empirically. We argue that a specification that explicitly allows arrivals of left and right jumps to differ is necessary.

References

Aït-Sahalia, Y., M. Karaman, and L. Mancini, 2018, The Term Structure of Equity and Variance Risk Premia, *Swiss Finance Institute Research Paper Series No 18-37*.

Andersen, T. G., O. Bondarenko, and M. T. Gonzalez-Perez, 2015, Exploring return dynamics via corridor implied volatility, *The Review of Financial Studies* 28, 2902–2945.

Andersen, T. G., N. Fusari, and V. Todorov, 2015, The risk premia embedded in index options, *Journal of Financial Economics* 117, 558–584.

Andersen, T. G., N. Fusari, and V. Todorov, 2017, Short-Term Market Risks Implied by Weekly Options, *The Journal of Finance* 72(3), 1335–1386.

Andersen, T. G., N. Fusari, and V. Todorov, 2019, The Pricing of Tail Risk and the Equity Premium: Evidence From International Option Markets, *Journal of Business & Economic Statistics*.

Bakshi, G., N. Kapadia, and D. Madan, 2003, Stock Return Characteristics, Skew Laws, and Differential Pricing of Individual Equity Options, *Review of Financial Studies* 16, 101–143.

Baltussen, G., S. van Bekkum, and B. van der Grient, 2018, Unknown Unknowns: Uncertainty About Risk and Stock Returns, *Journal of Financial and Quantitative Analysis* 53, 1615–1651.

Bardgett, C., E. Gourier, and M. Leippold, 2016, Inferring volatility dynamics and risk premia from the S&P500 and VIX markets, *Swiss Finance Institute Research Paper Series N13-40*.

Barndorff-Nielsen, O., N. Shephard, and M. Winkel, 2006, Limit theorems for multipower variation in the presence of jumps, *Stochastic Processes and their Applications* 116, 796–806.

Barndorff-Nielsen, O. E., and A. Veraart, 2012, Stochastic Volatility of Volatility and Variance Risk Premia, *Journal of Financial Econometrics* 11, 1–46.

Bates, D., 2000, Post-'87 Crash Fears in the S&P Futures Option Market, *Journal of Econometrics* 94, 181–238.

Bollerslev, T., and V. Todorov, 2014, Time-varying jump tails, *Journal of Econometrics* 183, 168–180.

Bollerslev, T., V. Todorov, and L. Xu, 2015, Tail risk premia and return predictability, *Journal of Financial Economics* 118, 113–134.

Bondarenko, O., 2014, Variance trading and market price of variance risk, *Journal of Econometrics* 180, 81–97.

Carr, P., and L. Wu, 2003, What type of process underlies options? A simple robust test, *Journal of Finance* 58, 2581–2610.

Carr, P., and L. Wu, 2017, Leverage Effect, Volatility Feedback, and Self-Exciting Market Disruptions, *Journal of Financial and Quantitative Analysis* 52, 2119–2156.

Duffie, D., J. Pan, and K. Singleton, 2000, Transform Analysis and Asset Pricing for Affine Jump-Diffusions, *Econometrica* 68, 1343–1376.

Eraker, B., 2004, Do Stock Prices and Volatility Jump? Reconciling Evidence from Spot and Option Prices, *Journal of Finance* 59, 1367–1403.

Eraker, B., M. Johannes, and N. Polson, 2003, The Impact of Jumps in Volatility and Returns, *Journal of Finance* 58, 1269–1300.

Hollstein, F., and M. Prokopczuk, 2018, How Aggregate Volatility-of-Volatility Affects Stock Returns, *The Review of Asset Pricing Studies* 8, 253–292.

Huang, D., C. Schlag, I. Shaliastovich, and J. Thimme, forthcoming, Volatility-of-Volatility Risk, *Journal of Financial and Quantitative Analysis*.

Jiang, G., and Y. Tian, 2005, The Model-Free Implied Volatility and Its Information Content, *Review of Financial Studies* 18, 1305–1342.

Jiang, G., and Y. Tian, 2007, Extracting Model-Free Volatility from Option Prices: An Examination of the VIX Index, *Journal of Derivatives* 14, 1–26.

Kaeck, A., 2018, Variance-of-Variance Risk Premium, *Review of Finance* 22, 1549–1579.

Kaeck, A., and C. Alexander, 2013, Continuous-time VIX dynamics: On the role of stochastic volatility of volatility, *International Review of Financial Analysis* 28, 46–56.

Kozhan, R., A. Neuberger, and P. Schneider, 2013, The Skew Risk Premium in the Equity Index Market, *Review of Financial Studies* 26, 2174–2203.

Pan, J., 2002, The Jump-Risk Premia Implicit in Options: Evidence from an Integrated Time-Series Study, *Journal of Financial Economics* 63, 3–50.

Park, Y., 2015, Volatility-of-volatility and tail risk hedging returns, *Journal of Financial Markets* 26, 38–63.

Figures and Tables

Figure 1. Time-Series of S&P 500 and Realized Volatility

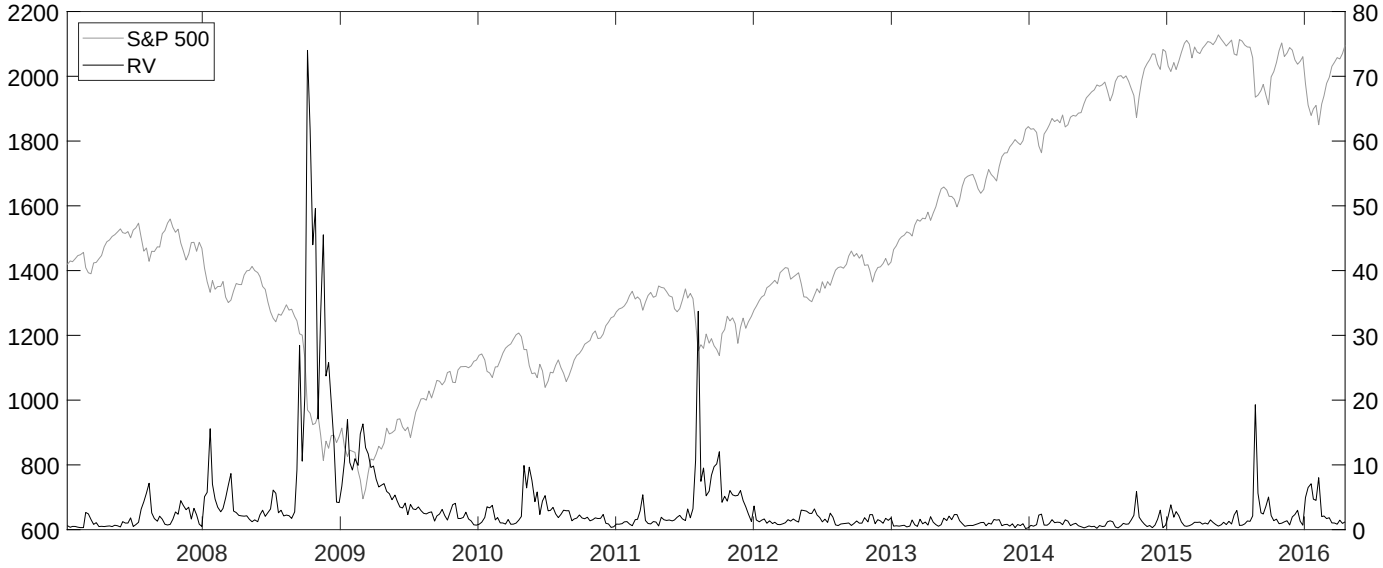

The figure shows weekly averages of the S&P 500 (left axis) and its realized volatility (right axis) for the years 1996 to April 2016. The realized volatility is calculated as the sum of squared 5-minute returns.

Figure 2. SPXW Option Implied Volatilites in June 2015 and January 2016

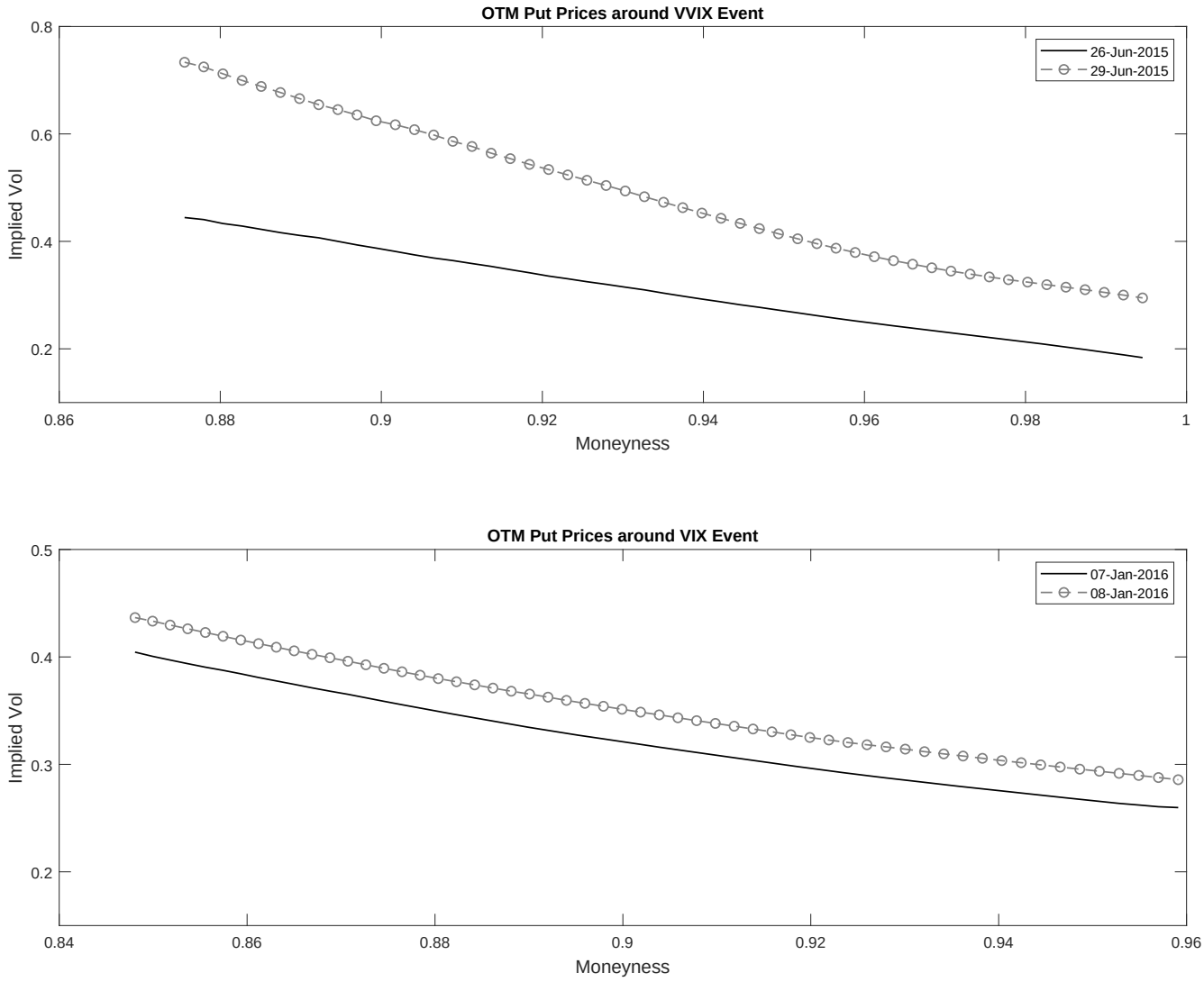

The figure depicts the change in implied volatilities over two events in June 2015 (upper plot) and January 2016 (lower plot). The implied volatilities are quoted by OptionMetrics and extracted from short-term SPXW (weeklys) put options. Moneyness is defined as $m = K/S$.

Figure 3. Time-Series of LJV compared to other Risk Measures

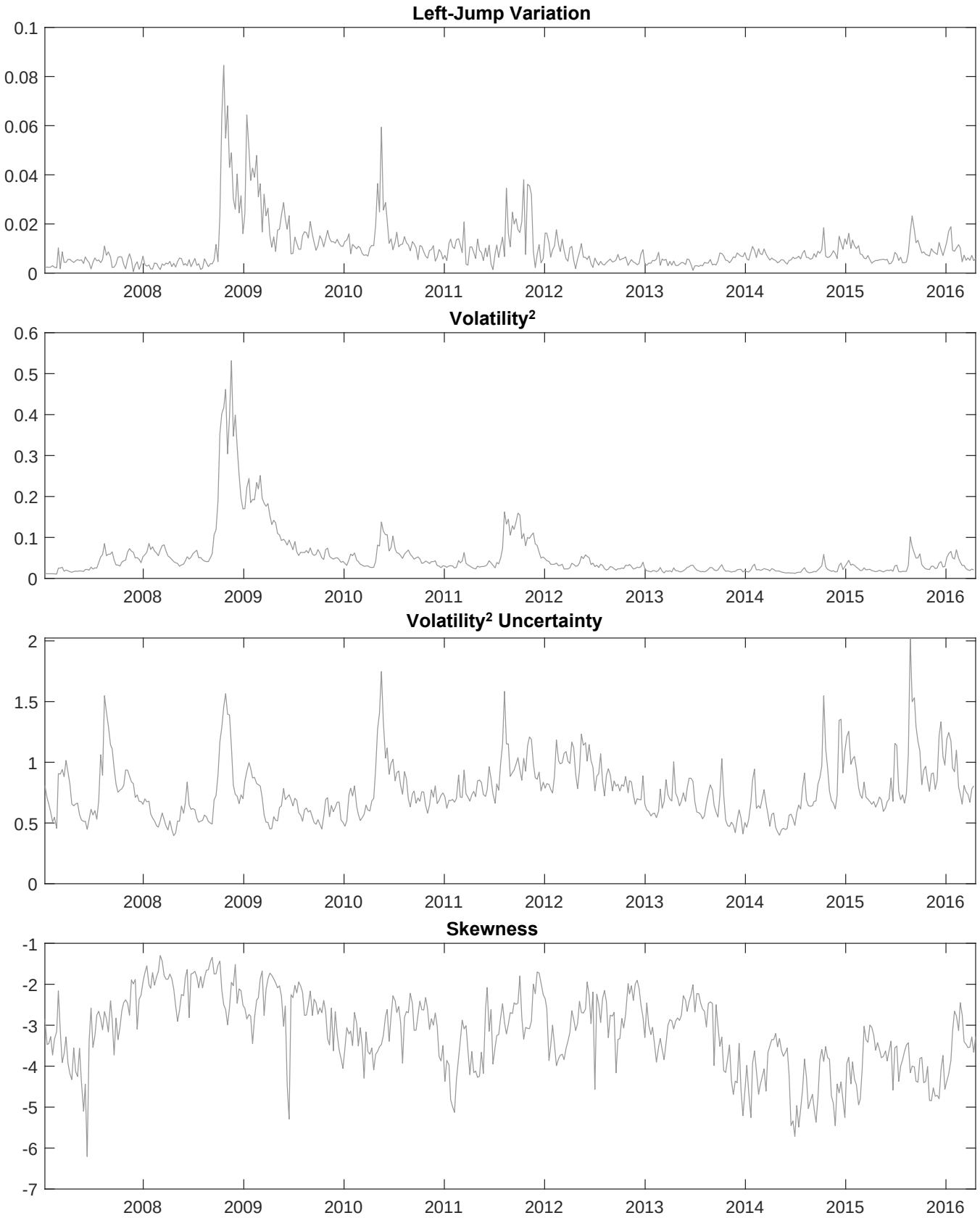

The figure shows the weekly average of left-tail risk (LJV), volatility, volatility uncertainty, and skewness for the years 1996 to April 2016. Section 2 describes the calculation of the measures.

Figure 4. Time-Series of RJV compared to other Risk Measures

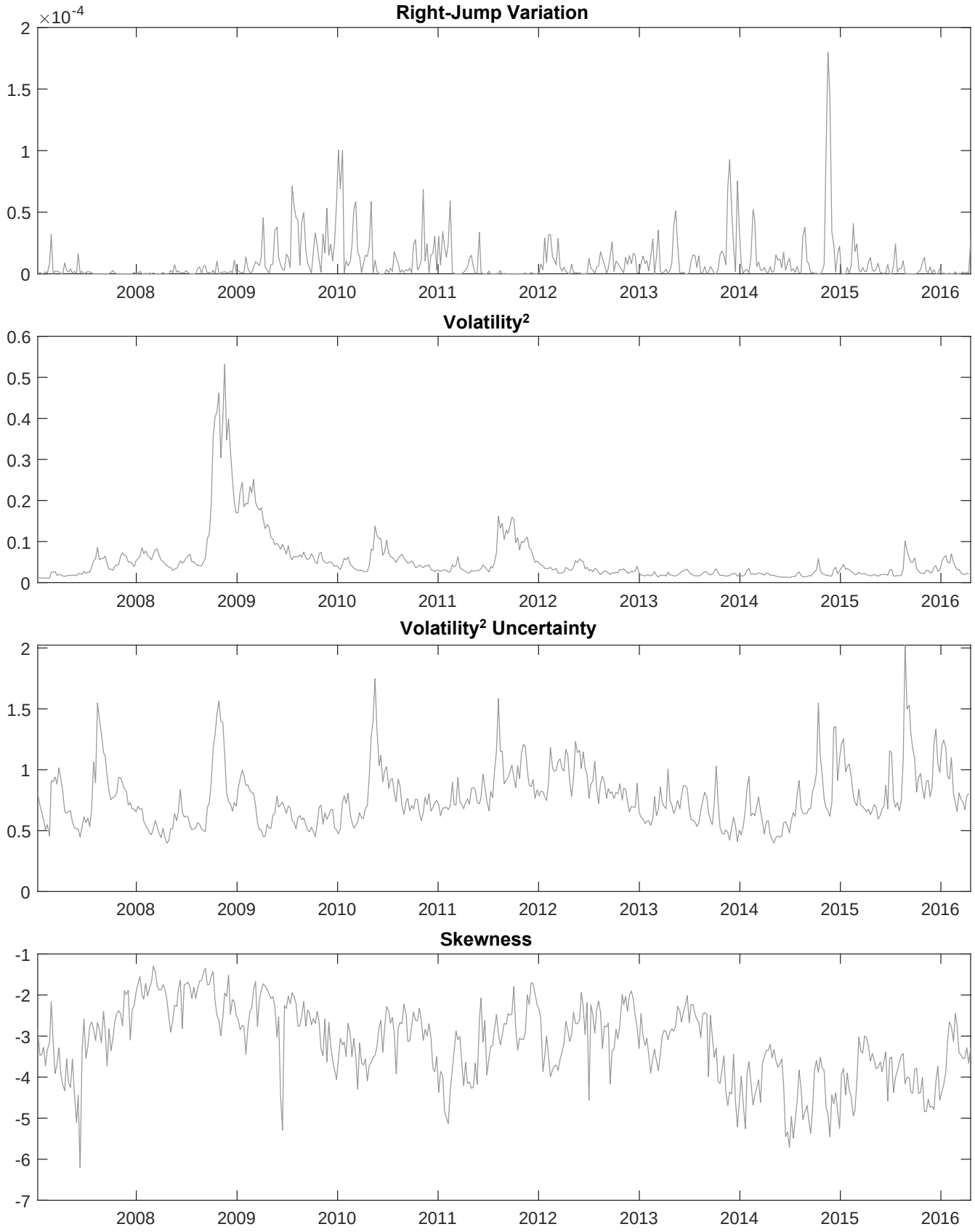

The figure shows the weekly average of right-tail risk (RJV), volatility, volatility uncertainty, and skewness for the years 1996 to April 2016. Section 2 describes the calculation of the measures.

Figure 5. Predictive Regressions - Adjusted R^2 and T-Statistic

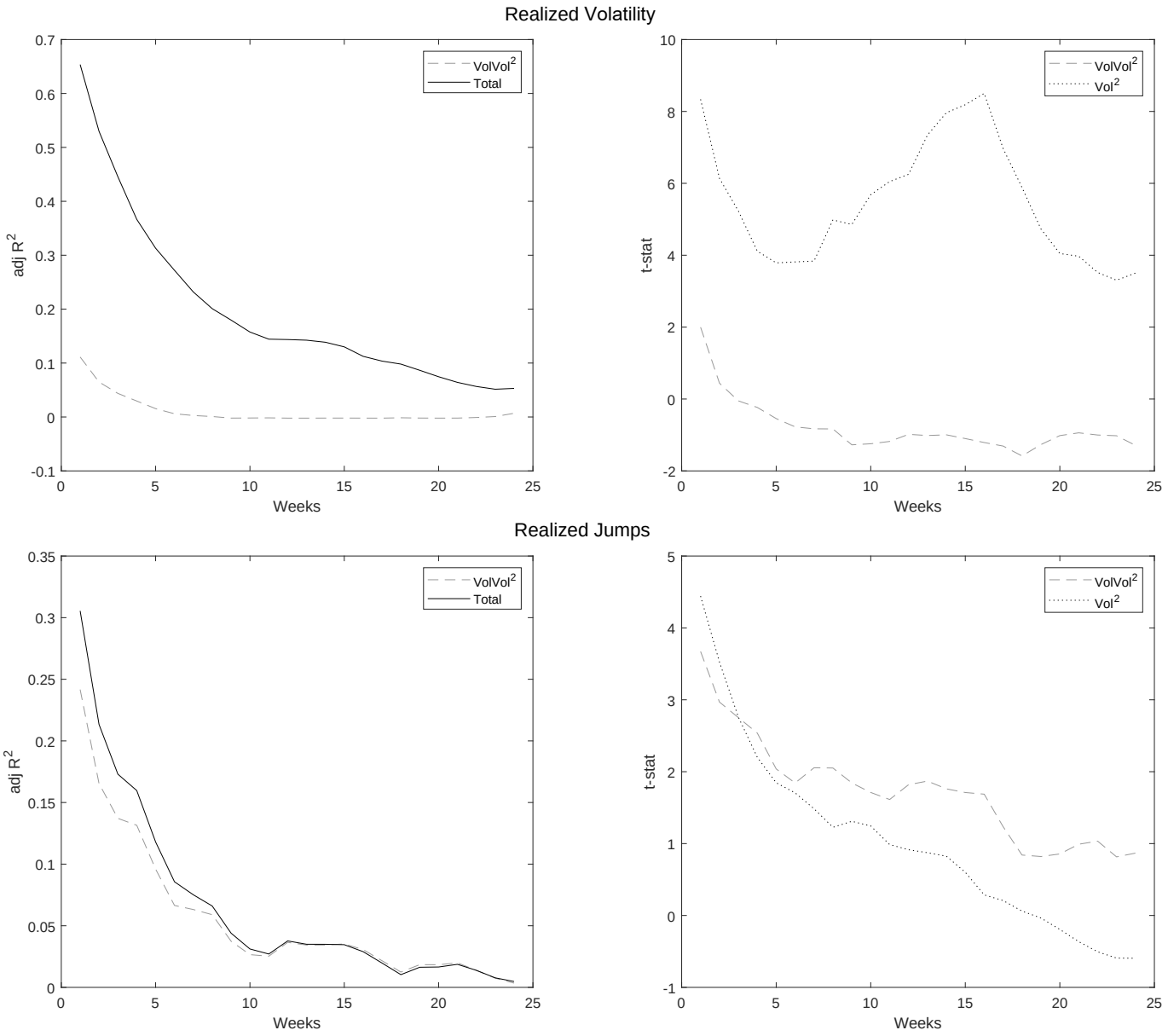

The figure shows adjusted R^2 (left panel) and t-statistics (right panel). We forecast realized volatility (top) and realized jumps (bottom) using volatility, volatility uncertainty, or both as predictors. The full drawn line in the left panel shows the total explained variation whereas the dashed line depicts the part explained by volatility uncertainty alone. The t-statistics are calculated with Newey-West standard errors.

Table I. Liquidity of SPX Options

$m \in$	$(-\infty, -4]$	$(-4, -2.5]$	$(-2.5, -1]$	$(-1, 1]$	$(1, 2.5]$	$(2.5, 4]$	$(4, \infty)$
Volume[#]	0.10	0.02	0.02	0.05	0.02	0.01	0.04
Volume[$]	0.96	0.21	0.40	1.18	0.32	0.13	0.32
$\widehat{\text{Volume}}$[%]	0.36	0.07	0.09	0.20	0.09	0.06	0.13
$\widetilde{\text{Volume}}$[%]	0.39	0.06	0.08	0.20	0.08	0.06	0.13
Open Interest[#]	1.25	0.15	0.18	0.25	0.16	0.13	0.41
Open Interest[$]	43.55	3.80	4.69	6.97	4.34	3.32	21.58
Open $\widehat{\text{Interest}}$[%]	0.47	0.06	0.08	0.11	0.07	0.06	0.16
Open $\widetilde{\text{Interest}}$[%]	0.52	0.06	0.07	0.10	0.06	0.05	0.14
Bid-$\widehat{\text{Ask Spread}}$	0.21	0.07	0.06	0.06	0.08	0.15	0.25
Bid-$\widetilde{\text{Ask Spread}}$	0.04	0.04	0.04	0.05	0.06	0.07	0.05

The table shows descriptives for daily liquidity measures of SPX options across different moneyness buckets. The quantities for Volume and Open Interest are quoted in millions. # refers to the absolute number of contracts, $ refers to the corresponding dollar value and % refers to the relative number of traded or open contracts. The Bid-Ask Spread is calculated as $2\,(\text{Ask} - \text{Bid}) \,/\, (\text{Ask} + \text{Bid})$. $\widehat{\bullet}$ and $\widetilde{\bullet}$ are the mean and median operator, respectively.

Table II. Descriptive Statistics

Panel A: Levels

	LJV	RJV	VolVol^2	Vol^2	SKEW
LJV	1				
RJV	0.03	1			
VolVol^2	0.43	−0.23	1		
Vol^2	0.79	−0.12	0.32	1	
SKEW	0.07	−0.23	−0.05	0.38	1
Mean	0.01	0.00	0.78	0.05	−3.18
Std	0.01	0.00	0.24	0.06	0.93
AC	0.79	0.60	0.82	0.95	0.82

Panel B: Difference

	LJV	RJV	VolVol^2	Vol^2	SKEW
LJV	1				
RJV	0.14	1			
VolVol^2	0.29	−0.12	1		
Vol^2	0.26	−0.05	0.44	1	
SKEW	−0.15	−0.12	0.10	0.10	1
Mean	0.00	0.00	0.00	0.00	0.00
Std	0.01	0.00	0.14	0.02	0.56
AC	−0.33	−0.15	−0.06	−0.11	−0.27

The table shows descriptive statistics for our option-implied risk measures from Section 2. Panel A shows correlations, mean, standard deviation (std) and autocorrelation (AC) for the weekly levels and Panel B for the weekly difference.

Table III. Regression Results - Δ Left Jump Variation

	(1)	(2)	(3)	(4)	(5)
ΔVol^2	0.2578		0.1954		0.2241
	(1.67)		(1.41)		(1.63)
ΔVolVol^2		0.2943			
		(3.44)			
$\Delta\text{VolVol}^{2,\perp}$			0.2025	0.3156	0.2303
			(3.01)	(4.22)	(3.30)
ΔSKEW				-0.2061	-0.2652
				(-4.66)	(-4.75)
adj. R^2	0.0644	0.0845	0.0996	0.1153	0.1345

The table shows results for the regressions with left-jump variation as dependent variable. All input variables are weekly averages and normalized by their full-sample standard-deviation. Newey-West robust t-statistics are given in the parentheses below. $\perp$ represents the orthogonal part.

Table IV. Regression Results - Δ Right Jump Variation

	(1)	(2)	(3)	(4)	(5)
ΔVol^2	-0.0515		-0.0097		-0.0090
	(-1.74)		(-0.46)		(-0.41)
ΔVolVol^2		-0.1220			
		(-3.17)			
$\Delta\text{VolVol}^{2,\perp}$			-0.1356	-0.1297	-0.1331
			(-3.09)	(-3.28)	(-3.05)
ΔSKEW				-0.1006	-0.0696
				(-1.88)	(-1.38)
adj. R^2	0.0006	0.0129	0.0153	0.0276	0.0248

The table shows results for the regressions with right-jump variation as dependent variable. All input variables are weekly averages and normalized by their full-sample standard-deviation. Newey-West robust t-statistics are given in the parentheses below. $\perp$ represents the orthogonal part.

Table V. Robustness Checks

	ΔLJV		ΔRJV	
	(1)	(2)	(3)	(4)
ΔVol^2	0.2359	0.1987	0.0323	-0.0086
	(1.07)	(1.42)	(0.49)	(-0.40)
$\Delta\text{VolVol}^{2,\perp}$	0.1857	0.2060	-0.1803	-0.1344
	(2.66)	(3.04)	(-2.77)	(-3.05)
ΔKURT		0.0551		-0.0086
		(2.34)		(0.44)
adj. R^2	0.1383	0.1008	0.0205	0.0136

The table shows regression results for the subsample 2010 - 2016 in column (1) and (3) as well as for full sample with Kurtosis as additional independent variable in column (2) and (4). All input variables are normalized by their full-sample standard-deviation. Newey-West robust t-statistics are given in the parentheses below. $\perp$ represents the orthogonal part.

Table VI. Regression Results - Model of Eraker (2004)

	ΔLJV			ΔRJV		
	(1)	(2)	(3)	(4)	(5)	(6)
ΔVol^2	0.8102		0.8115	0.1248		0.1254
	(3.49)		(3.61)	(1.92)		(1.99)
ΔVolVol^2		-0.3104			-0.0835	
		(-4.77)			(-1.99)	
$\Delta\text{VolVol}^{2,\perp}$			-0.1015			-0.0525
			(-2.45)			(-1.40)
adj. R^2	0.6557	0.0945	0.6654	0.0136	0.0049	0.0143

The table shows regression results for model-implied risk measures. All input variables are normalized by their full-sample standard-deviation. Newey-West robust t-statistics are given in the parentheses below. $\perp$ represents the orthogonal part.

Table VII. Regression Results - Model of Kaeck (2018)

	ΔLJV			ΔRJV		
	(1)	(2)	(3)	(4)	(5)	(6)
ΔVol^2	-0.0094		-0.0449	0.0635		0.0268
	(-1.38)		(-2.50)	(1.22)		(0.51)
ΔVolVol^2		0.1634			0.1818	
		(2.10)			(2.06)	
$\Delta\text{VolVol}^{2,\perp}$			0.1670			0.1906
			(2.08)			(2.10)
adj. R^2	-0.0017	0.1231	0.1213	0.0045	0.0728	0.0811

The table shows regression results for model-implied risk measures. All input variables are normalized by their full-sample standard-deviation. Newey-West robust t-statistics are given in the parentheses below. $\perp$ represents the orthogonal part.